Absolute single and multiple charge exchange cross sections for highly charged C, O, and Ne ions on H_2O, CO, and CO_2

R. J. Mawhorter,[1,2] A. Chutjian,[1] T. E. Cravens,[3] N. Djurić,[1] S. Hossain,[1] C. M. Lisse,[4] J. A. MacAskill,[1] S. J. Smith,[1] J. Simcic,[1] and I. D. Williams[5]

[1]*Jet Propulsion Laboratory, California Institute of Technology, Pasadena, California 91109, USA*
[2]*Department of Physics & Astronomy, Pomona College, Claremont, California 91711, USA*
[3]*Department Physics and Astronomy, University of Kansas, Lawrence, Kansas 66045, USA*
[4]*Space Department, Johns Hopkins University, Applied Physics Laboratory, Laurel, Maryland 20723, USA*
[5]*Physics Department, The Queen's University, Belfast BT7 1NN, United Kingdom*

(Received 12 October 2006; revised manuscript received 4 January 2007; published 6 March 2007)

Reported herein are measured absolute single, double, and triple charge exchange (CE) cross sections for the highly charged ions (HCIs) C^{q+} ($q=5,6$), O^{q+} ($q=6,7,8$), and Ne^{q+} ($q=7,8$) colliding with the molecular species H_2O, CO, and CO_2. Present data can be applied to interpreting observations of x-ray emissions from comets as they interact with the solar wind. As such, the ion impact energies of $7.0q$ keV (1.62–3.06 keV/amu) are representative of the fast solar wind, and data at $1.5q$ keV for O^{6+} (0.56 keV/amu) on CO and CO_2 and $3.5q$ keV for O^{5+} (1.09 keV/amu) on CO provide checks of the energy dependence of the cross sections at intermediate and typical slow solar wind velocities. The HCIs are generated within a 14 GHz electron cyclotron resonance ion source. Absolute CE measurements are made using a retarding potential energy analyzer, with measurement of the target gas cell pressure and incident and final ion currents. Trends in the cross sections are discussed in light of the classical overbarrier model (OBM), extended OBM, and with recent results of the classical trajectory Monte Carlo theory.

DOI: 10.1103/PhysRevA.75.032704 PACS number(s): 34.50.Gb, 82.30.Fi, 96.60.Vg

I. INTRODUCTION

Charge exchange (CE) of highly charged ions (HCIs) with neutral atomic and molecular species is a dominant process that occurs in a variety of high electron temperature plasmas. These plasmas include fusion devices [1–3], various astrophysical regions involving the interaction of HCIs (as solar and stellar winds, or as magnetospherically confined ions) with cometary neutral species [4–7], circumstellar neutral clouds [8], and planetary atmospheres [9,10]. A summary of abundance of the HCIs in the solar wind [11] is given in Fig. 1. One sees that the most important solar wind species include $C^{(5,6)+}$, N^{5+}, $O^{(6-8)+}$, and Ne^{8+}, for which the current paper presents absolute charge exchange cross sections. An important diagnostic of CE in these plasmas is the observation of x-ray emission following the electron transfer into high-n orbitals of the HCI projectile, and subsequent radiative decays in the x-ray spectral region [6,12].

Recent CE cross sections and n-state distributions have been reported for N^{7+}, O^{7+} ions colliding with H_2O, CO_2, and CO [13]; and Ne^{10+} ions with He, Ne, Ar, CO, and CO_2 [14]. Comparisons have been given with results in the classical trajectory Monte Carlo (CTMC) model, the Landau-Zener (LZ) approximation [15–18], and the classical overbarrier model (OBM) [19–21]. Cross sections for CE of C^{q+} ions (for ion charge $q=1-4$) with H_2, CH_4, C_2H_6, C_3H_8, and CO_2 have been reported and discussed in light of the incident ion-energy dependence, scaling laws, and target ionization potentials [22].

Theoretical approaches that have allowed a direct comparison with fusion and astrophysical ion-neutral systems are the CTMC, molecular-, and atomic-orbital close-coupling methods, and the continuum distorted-wave method [18,22–24]. Theoretical work has progressed in calculating transition probabilities and branching ratios; and the underlying database of CE cross sections and x-ray emission spectra has increased. These have led to an emphasis on determining specific (n,l) state distributions following electron capture. The resulting cascade processes have been modeled with comparisons to both laboratory [25] and solar-system [10,26,27] x-ray spectra.

Presented herein are absolute single and multiple CE cross sections for various charge states of C, N, O, and Ne ions colliding with molecular targets. The goal of this work is to benchmark results of theoretical calculations, and to provide needed data in the areas of comet, planetary, circumstellar, and fusion physics. The experimental approach for generating the HCIs of known charge-to-mass, charge exchanging with the neutral species, measuring the ion charges

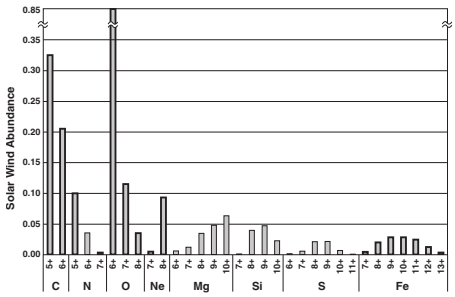

FIG. 1. Ion species and their abundance in the solar wind [11]. Shown are the average of the abundance in the fast and slow components of the solar wind, all relative to the summed $O^{(5-8)+}$ ion abundances. Other abundances (not displayed) are $H^+=1600$ and $He^{2+}=70$. Histogram bars shown in bold outline indicate species for which CE cross sections have been measured at JPL.

and currents after the collision, and error determination is discussed in Sec. II. Results are given in Sec. III and discussed in light of previous experimental data, and of theoretical results in the CTMC and classical and extended OBM models. Conclusions and a view towards future work are given in Sec. IV.

II. EXPERIMENTAL CONSIDERATIONS

The experimental study uses the electron cyclotron resonance (ECR) ion source and the CE x-ray detection beam line at the JPL Highly Charged Ion Facility. Details of the beam lines [28], the CE geometry, system calibration, and errors [29–32] have been given previously, and only subsequent changes are discussed in the following.

Prior to the start of the measurements a LabView data acquisition system was assembled and programmed. This system makes use of the current-sampling protocol available with the Keithley 6514 digital electrometer, improving statistical errors and streamlining the data-taking process which is now under personal-computer control.

In terms of the CE gas cell, all measurements were taken with the largest cell exit aperture diameter possible (4.09 mm) consistent with maintaining good pressure within the cell, and limiting the pressure gradient towards the ion exit region. Such gradients introduce the possibility of CE outside the geometric limits of the cell, and hence add uncertainty to the effective path length of the cell, and to the final absolute cross section.

In a separate study the effect of aperture diameters was examined in greater detail on the more challenging cases of $^3He^{2+}$ charge exchanging with He and H_2 [55]. The scattering kinematics of light ions incident on light targets results in the largest angular spread in the CE products, especially for the exothermic case of the partners $^3He^{2+}+He$. The 4.09 mm diameter exit aperture results in an acceptance half angle of 1.93°, yielding a collection efficiency for scattering from H_2 of 98–99%; and a collection efficiency of about 90% for scattering from He, with efficiencies depending on the incident ion energy. A detailed model of the cell, and corrections for the uncollected ions for these limiting cases can be calculated using differential cross sections [33,34]. These results are in excellent agreement with the experimental study of Kusakabe *et al.* [35] using an acceptance half angle of 2.50°. A comparison with a low-energy (up to 430 eV), two-channel radial coupling calculation [36] in the system $C^{6+}+H$ shows that the collection angle effects are negligible, and that essentially the full collection of CE products was achieved in the present and previous JPL studies.

In any study using an ECR ion source it is important to consider the role of metastable ions in the parent beam, and indeed the present 14 GHz ECR source has been used to measure metastable ion lifetimes in oxygen and iron ions [37,38]. The extent to which the presence of metastable ions will affect a CE measurement depends on both the metastable population and its CE cross section relative to that of the ground state. As in previous studies (see Ref. [32] for a detailed discussion), tests were carried out herein to examine the sensitivity of cross section to metastable ions.

One test of metastable content involves running the ECR plasma chamber in "low pressure" ($\approx 2\times10^{-5}$ Pa) and "high pressure" ($\approx 7\times10^{-5}$ Pa) modes, and comparing cross section results for a given ion-molecule pair [32]. Using a second beam line [28] one is able to trap all ions in the Kingdon ion trap and monitor the emitted photons from a metastable level. In a second test, one can introduce a quenching gas (N_2 or Ar) into a long section of the beam line between the 90° charge/mass selection magnet and the electrostatic "Y" deflector [28]. In both tests the ECR and beam-line gas-pressure conditions can be adjusted to reduce the metastable-level photon emission intensity in the trap to below its detection limit.

Additionally, a separate series of measurements using the beam attenuation method [32,39–41] was used as a diagnostic of metastable content. This was done by varying the pressure of Ar in the CE gas cell, and monitoring the decreasing transmission of the ions, with break points, as a function of increasing Ar pressure. A summary of the metastable diagnostics is given in Ref. [32]. In sum, these diagnostics served to exclude the effects of metastable HCI states in the cross section determinations.

The errors in this study are described in detail in recent Fe^{q+}-He CE results [32]. An error propagation was performed by adding the 2σ statistical errors, taking into account the number of measurements for each ion-molecule pair, in quadrature with the errors in measuring the gas density, ion current ratios, absolute currents, ion beam instabilities, and the effective gas-cell collision length (including a correction for gas streaming) of 7.2%. Use of the digital electrometer led to an improved signal sampling and a direct digital output which improved the statistical error. The final convoluted 2σ errors in the data are listed for each measurement in Table I. These errors averaged to 8% ($\sigma_{q,q-1}$), 12% ($\sigma_{q,q-2}$), and 20% ($\sigma_{q,q-3}$).

III. RESULTS AND DISCUSSION

Shown in Table I are the present single ($\sigma_{q,q-1}$), double ($\sigma_{q,q-2}$), and triple ($\sigma_{q,q-3}$) CE cross sections for the indicated charge states of C, O, and Ne ions colliding with the molecular targets CO, CO_2, and H_2O. (These targets comprise a subset of the most important comet species, with additional targets being H, C, O, and OH.) All data are displayed in Figs. 2–5, along with results of the OBM and CTMC calculations where available. Prior to obtaining the experimental results, a series of measurements overlapping the earlier data of Ref. [31] was undertaken. This served as a consistency check, especially of the digital electrometer, the data-acquisition software, and the angular-collection effects of the larger exit aperture in the CE cell. All present and earlier [31] data are displayed in Figs. 2–5. Data for single CE are considered first, followed by multiple exchange results, and energy dependences in the cross sections.

A. Single charge exchange results

The $\sigma_{q,q-1}$ results for target molecules CO_2 and CO are shown in Fig. 2. Because the ionization potential (I_P) of CO_2

TABLE I. Absolute single and multiple charge exchange cross sections for $C^{(3,5,6)+}$, $O^{(5,6,7,8)+}$, and $Ne^{(7,8)+}$ ions colliding with CO, CO_2, and H_2O. The ionization potential (I_P) is given in the first column for each species. All cross sections are in units of 10^{-15} cm^2.

		Projectile											
		C^{3+}	C^{5+}	C^{6+}	O^{5+}		O^{6+}		O^{7+}	O^{8+}	Ne^{7+}	O^{8+}	
Target / I_P		fast[a]	fast[a]	fast[a]	fast[a]	slow[b]	fast[a]	slow[c]	fast[a]	fast[a]	fast[a]	fast[a]	
CO	$\sigma_{q,q-1}$	1.20±0.09	4.16±0.32	5.54±0.44	4.33±0.32	4.36±0.33	5.11±0.40	5.59±0.44	6.58±0.49	6.31±0.53	6.85±0.55	7.85±0.61
14.01 eV	$\sigma_{q,q-2}$	…	0.69±0.08	1.01±0.20	0.57±0.08	0.54±0.04	0.97±0.12	1.12±0.10	1.19±0.10	1.58±0.41	1.66±0.19	1.71±0.14
	$\sigma_{q,q-3}$	…	…	…	…	0.43±0.05	…	0.38±0.06	0.14±0.08	0.62±0.31	0.44±0.13	0.38±0.03
CO_2	$\sigma_{q,q-1}$	…	…	…	3.82±0.30	…	4.83±0.37	5.60±0.45	5.53±0.55	…	6.08±0.56	7.74±0.63
13.77 eV	$\sigma_{q,q-2}$	…	…	…	0.77±0.13	…	1.36±0.12	1.37±0.11	1.30±0.14	…	2.16±0.17	1.86±0.15
	$\sigma_{q,q-3}$	…	…	…	…	…	0.38±0.05	0.47±0.04	0.41±0.07	…	0.47±0.06	0.71±0.06
H_2O	$\sigma_{q,q-1}$	…	4.17±0.32	…	…	…	5.29±0.40	…	…	…	5.46±0.41	8.71±0.77
12.62 eV	$\sigma_{q,q-2}$	…	0.60±0.10	…	…	…	0.81±0.07	…	…	…	1.19±0.13	1.73±0.19
	$\sigma_{q,q-3}$	…	…	…	…	…	0.35±0.03	…	…	…	0.54±0.10	0.42±0.06

[a]Corresponding to an acceleration voltage of 7.0 kV.
[b]Corresponding to an acceleration voltage of 3.5 kV.
[c]Corresponding to an acceleration voltage of 1.5 kV.

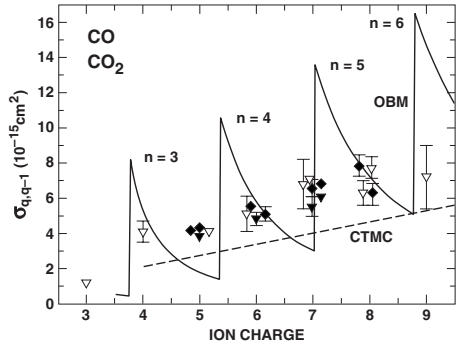

FIG. 2. Absolute single CE cross sections (the sum of single capture and autoionizing double capture events) for highly charged ions with CO and CO_2. All values in Figs. 2–5 are listed in Table I herein and in Ref. [31]. Some data points have been slightly displaced along the charge axis, and some error bars removed for clarity. Comparisons are given to results in the classical over-barrier model [19–21], and to CTMC results [23]. The legend is as follows: ◆, C^{q+}, O^{q+}, Ne^{q+} on CO; ▼, C^{q+}, O^{q+}, Ne^{q+} on CO_2; ▽, $C^{3,6+}$, $N^{4,7+}$, $O^{5,7,8+}$, Ne^{9+} on CO_2 (from Ref. [31]).

(13.78 eV) is close to that of CO (14.01 eV), the $\sigma_{q,q-1}$ are expected to be similar on the basis of the OBM, in which the I_P is the only free parameter. The expression for the cross section in the OBM is obtained through the crossing radius R_c for hydrogenic systems, and is given as

$$R_C = \frac{q-1}{q^2/2n^2 - I_P}, \tag{1}$$

where n is the final principal quantum number, and the CE cross section is given by $\pi R_c^{\,2}$. Equation (1) can be a useful, first-order guide towards estimating single CE cross sections for unknown species, based only on their I_P's.

Referring to the $\sigma_{q,q-1}$ cross sections for O^{5+} and O^{7+} on CO_2 (Fig. 2), one sees that the present results agree with those of Ref. [31] to within the combined 2σ error limits. Indeed, all of the data in Fig. 2 for a given charge state

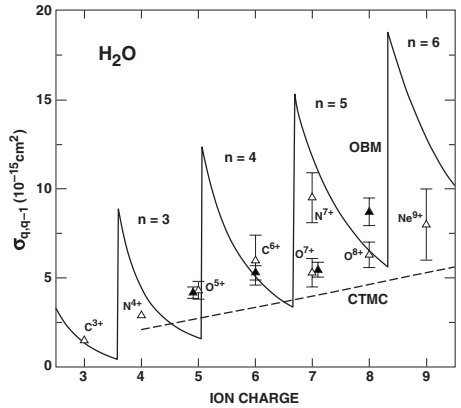

FIG. 3. Absolute single CE cross sections (the sum of single capture and autoionizing double capture events) for highly charged ions with water. Filled triangles (▲) are present data for C^{5+}, O^{6+}, Ne^{7+}, and Ne^{8+}. Open triangles (△) are data from Ref. [31] for the ions indicated. Comparisons are given to results in the classical over-barrier model [19–21], and to CTMC results [23].

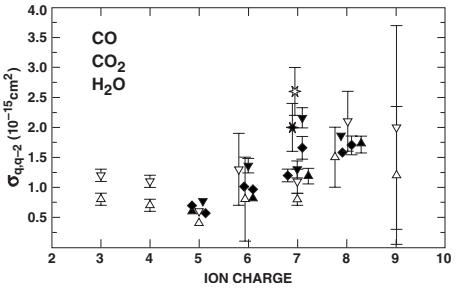

FIG. 4. Absolute double CE cross sections for CO, CO_2, and H_2O at an ion acceleration potential of 7 kV. The legend is as follows: ◆, C^{q+}, O^{q+}, Ne^{q+} on CO; ▼, C^{q+}, O^{q+}, Ne^{q+} on CO_2; ▲, C^{q+}, O^{q+}, Ne^{q+} on H_2O; ▽, C^{q+}, N^{4+}, O^{q+}, Ne^{q+} on CO_2 (from Ref. [31]); △, C^{q+}, N^{4+}, O^{q+}, Ne^{q+} on H_2O (from Ref. [31]); ☆, N^{7+} on CO_2 (from Ref. [31]); ★, N^{7+} on H_2O (from Ref. [31]).

cluster together and exhibit a uniform trend of increasing cross section with ion charge q. This is supported theoretically by both the OBM and CTMC results [23], with good agreement in slope for the more sophisticated CTMC calculation. As expected the cusps of the OBM are not observed experimentally, and are an indication that electron capture is occurring into a range of final-state projectile n levels rather than into a single n level.

Shown in Fig. 3 are absolute single CE results for C, N, O, and Ne ions colliding with H_2O (I_P=12.62 eV). The trend of increasing cross section with q is maintained up to the highest level studied (q=9). The dependence (or lack thereof) on I_P is established by comparison with unpublished CE measurements with CH_4 as the target [42]. The I_P of CH_4 is 12.99 eV, close to that of H_2O, and it is found that the CH_4 cross sections agree well with the H_2O results for $q \leqslant 6$, and straddle the three cross section values for N^{7+}, O^{7+}, and Ne^{7+}. The trend of increasing single exchange cross section with increasing charge is also seen in the CTMC calculation with comparison to data for H_2O, CH_4, and CO_2 (see Fig. 5 of Ref. [23]).

There is a consistent positive offset of all measured data above the CTMC by typically 15–50 %. This was also the case for earlier CTMC calculations for O^{8+} and Ne^{10+} [23]. One source of the discrepancy could lie in the fact that present experiments also include effects of autoionizing multiple captures to adjacent energy levels (leaving just a single electron captured), and hence contribute to the true single capture cross section. The CTMC includes only the direct single electron capture (SEC), and thus would be an underestimate to the sum of all direct and indirect paths leading to $\sigma_{q,q-1}$. In addition, assuming that the classical nature of CTMC is not the limiting factor at these collision energies, the offset may lie in the assumption that there is only one active electron. For example, Hasan *et al.* [13] use the CTMC to calculate the average n for SEC in He, CO, CO_2, and H_2O for the projectiles N^{7+} and O^{7+}. While these CTMC cross sections are consistently low, the best value is for fast N^{7+} on He, where the assumption of one active electron becomes more reasonable.

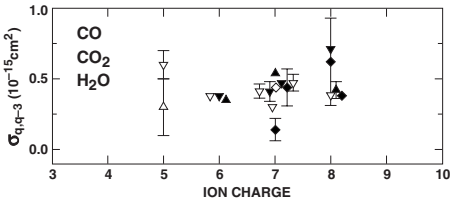

FIG. 5. Absolute triple CE cross sections for CO, CO_2, and H_2O at an ion acceleration potential of 7 kV. The legend is as follows: ◆, O^{q+}, Ne^{q+} on CO; ▼, O^{q+}, Ne^{q+} on CO_2; ▲, O^{q+}, Ne^{q+} on H_2O; ▽, O^{q+} on CO_2 (from Ref. [31]); △, O^{q+} on H_2O (from Ref. [31]).

B. Multiple charge exchange results

As has been pointed out in recent publications [13,23,25], multiple electron exchanges play a noticeable role in the modeling of x-ray emissions from cometary systems. Experimentally, the measurement of double and triple CE cross sections (which include all indirect capture-autoionization paths) is more difficult due to the lower outgoing ion currents involved. Shown in Figs. 4 and 5 are the present results for the absolute double and triple CE cross sections for all 7.0 kV ion-molecule pairs studied herein, along with comparisons given to earlier data [31]. The present data, with 2σ error limits, are also listed in Table I. An enticing feature of the double CE cross sections in Fig. 4 is the noticeable undulation with respect to q. There is a consistent and significant minimum at q=5 for both C^{5+} and O^{5+} on any target, which might be the result of a loss of flux into the single and triple CE channels. Such an effect was observed in the single and double CE cross sections reported for the $Fe^{q+\text{-He}}$ system (see Fig. 3 of Ref. [32]). Noted there was a clear maximum in the double CE cross section for Fe^{6+}, accompanied by a minimum in the single CE cross section; and a maximum in the single CE cross section for Fe^{10+} with a minimum in the double exchange. This effect was ascribed to the varying contribution of the autoionizing double capture (ADC) channel to the single CE, where the competition between ADC and radiative stabilization will depend upon the initial $nl,n'l'$ capture states. The continued study of this possibility awaits improvements in the experimental technique, accompanied by refinements in the theory to include the many open capture-ionization channels.

Perhaps just as interesting is the phenomenon that for a number of charge states and ions the double-exchange CO_2 cross sections lie above the H_2O cross sections, with the CO cross section value lying between. The pattern is true for q =3–7, with the CO_2-H_2O differences being greater than 2σ. Given the inverse relationship between I_P and cross section, this is not expected on the basis of the first I_P values, but would be expected on the basis of the second I_P's. From Auger spectra these are known to be 24 eV for CO_2, 26 eV for CO, and 27 eV for H_2O [43]. The same trend and similar values can be arrived at by using Koopman's theorem on *ab initio* calculations on the corresponding singly charged ions [44,56]. The consistency of the experimental data and error limits is noteworthy, with the data having been acquired with different hardware and software over a period of about five years. The same trend is evident in the smaller triple exchange cross sections in Fig. 5.

Comparing the multiple and single exchange cross sections, it is interesting that the closely matching results for $q=5$ and $q=6$ differ at $q=7$ for single exchange on H_2O (Fig. 3). This is also seen in all double exchange results, with the N^{7+} results lying higher than the Ne^{7+} and O^{7+} cross sections (Fig. 4). But for the single exchange results (Figs. 2 and 3) the Ne^{8+} cross sections are somewhat larger than for O^{8+}, especially for H_2O. On average, for all targets and projectiles, the ratio of single to double CE cross sections is about 4.5, and that of double to triple about 2.8. It appears that inclusion of multiple CE data into models would be needed [14], especially if one were interested in obtaining plasma properties to an accuracy of 10–15%, consistent with spacecraft measurement accuracies. Furthermore, through single and sequential CE interactions the HCIs can be converted to lower charge states having large CE rate coefficients that can markedly affect the state of the plasma [45].

C. Energy dependence of the charge exchange results

Ions in the solar wind have a bimodal velocity distribution with comparable numbers of ions in both the fast and slow components [11]. In order to model the solar wind-comet interaction it is important to understand the dependence of CE cross section on projectile energy. In terms of the experimental parameters, an accelerating potential of 7.0 kV for an O^{7+} ion corresponds to an ion velocity of approximately 770 km/s (fast solar wind), 1.5 kV to 360 km/s (slow solar wind), with 3.5 kV (540 km/s) lying in between.

Examination of the $3.5q$ keV O^{5+} on CO results (Table I) shows that they are essentially identical to the $7.0q$ keV results. Results for lower-energy $1.5q$ keV O^{6+} ions colliding with CO and CO_2 are also similar to one another; they are also close to the corresponding $7.0q$ keV values, but show a slight trend towards higher cross sections with decreasing energy. One fairly close comparison is with the energy dependence among single, double, and triple exchange cross sections for C^{q+} ($q=1-4$) ions incident on several polyatomic molecules. Referring to Fig. 3 of Ref. [22], it is found that near 1 keV/amu (12 keV) the multiple CE cross sections are generally flat, or have a small positive or negative slope with energy. This was also noted in the CE studies of $He^{2+}+CO$ [46] and $He^{2+}+H_2O$ [47], where the slope for single exchange was positive, while that for double exchange was negative in this energy region. Another study [48] gave a similar behavior for single exchange by He^{2+} on CO_2, CH_4, CO, and H_2O. It is interesting to point out that the results for $He^{2+}+H_2O$ [47] are in excellent agreement with the study of Seredyuk *et al.* (see Fig. 5 in Ref. [49]). The single lowest-energy point in Ref. [46] that appears to be in disagreement is an extrapolated rather than measured point.

Lithiumlike O^{5+} was reported to have a metastable state with a measured lifetime of approximately 1 μs [50]. Although O^{5+} is not expected to have metastable levels, nevertheless data were taken at both high and low ECR pressure modes, and at acceleration potentials of 3.5 kV and 7.0 kV. The latter tests served to lengthen the flight time (5.9 μs vs 8.3 μs, or ~5.9 lifetimes to ~8.3 lifetimes) to allow the metastable ions more time to decay, albeit both flight times are already sufficiently long. Data were taken on the $O^{5+}+CO$ system at both potentials, and under high- and low-pressure conditions. No statistically significant trend in σ_{54} was detected either with flight time or quenching gas pressure, and hence the effect of any metastable level in O^{5+} was deemed negligible.

Finally, for the sake of completeness, a set of cross sections was calculated for the CO target using the extended overbarrier model (EOBM) [52] and the assumptions therein. The CO binding energies were taken from Refs. [53,54]. Calculated results for single-charge exchange cross sections for C^{5+} are 7.4 (units of 10^{-15} cm^2, see also Table I), with the predominant channel being a single electron transfer to the projectile; and 8.4 for C^{6+}, with the predominant channel again being a single electron transfer. Calculated results for double-charge exchange strings for C^{5+} are 0.62, with the predominant channel being three electron transfers and a single autoionization; and 1.2 for C^{6+}, with the predominant channel again being three electron transfers and a single autoionization. Thus, for the C^{5+} and C^{6+} projectiles the calculated single exchanges are overestimated relative to measurement by a factor of about 1.7, and the double exchanges are calculated to lie within about 15% of measurement. Analogous EOBM estimates were derived from strings for other collision partners in Table I, and these results will be reported in a future publication.

IV. CONCLUSIONS

Using the JPL Highly-Charged Ion Facility absolute single, double, and triple CE cross sections have been measured for C^{q+} ($q=3,5,6$), O^{q+} ($q=5-8$), and Ne^{q+} ($q=7,8$) ions colliding with CO, CO_2, and H_2O. Diagnostics were carried out in all cases for possible contributions from metastable levels. Good agreement is found with earlier measurements of Greenwood *et al.* [31], and measurements for CH_4 ($I_P=12.61$ eV) [42] agree well with data for H_2O (12.62 eV). All single exchange measurements are consistent with the trend of increasing single CE cross section with ion charge, in agreement with trends in the overbarrier and classical trajectory Monte Carlo models. However, data are 15–50% above the results for the CTMC model. An interesting minimum in the double CE cross section for all ions studied here and in Ref. [31] is observed at $q=5$, which may be an indication of flux from the autoionizing double capture channels directed towards the single ionization channel, as was observed in earlier studies for the Fe^{q+}-He system [32].

For most charge states in Figs. 2–5 there is a well-behaved clustering of cross sections that is essentially independent of the projectile ion. However, some persistent measured differences exist for $q=7$ and $q=8$. These could be explored by further studies of the nitrogen ions between N^{4+} and N^{7+}; to cover the charge range $q=8-10$ one would select from the unstudied Mg, Si, and S series (Fig. 1) to both provide data as well as establish trends. In terms of target gases, the agreement of the CO and CO_2 single CE cross sections coupled with the consistency exhibited for multiple exchange indicate that only one of this pair need be studied extensively, with spot checks for the other. In this regard,

given the importance of the I_P it would be interesting to add a low I_P molecule such as CH_3OH (I_P=10.84 eV) to one of the other middle-valued pair [I_P (H_2O)=12.62 eV, I_P (CH_4)=12.61 eV]. Indeed, first results using CH_3OH and CH_4 as targets are in preparation [42].

Finally, an assessment of measurements required for the comet x-ray problem is given, and suggestions can be made for data on the solar-wind ions N^{6+}, Mg^{q+} (q=6–10), Si^{q+} (q=7–10), and S^{q+} (q=6–11) charge exchanging with the comet neutral molecules. X-rays have also been observed at both Venus and Mars, and these HCIs participate in CE processes at Mars [51]. All results would benefit from additional theoretical inputs through extensions of the CTMC model and the multichannel Landau-Zener approximation [14].

ACKNOWLEDGMENTS

This work was carried out at the Jet Propulsion Laboratory, California Institute of Technology and was supported through agreement with the National Aeronautics and Space Administration. S.H. and J.S. acknowledge the support of the NASA Postdoctoral Program. Thanks are due to W. Steinmetz for carrying out the *ab initio* second ionization potential calculations and to J. B. Greenwood for helpful discussions.

[1] P. G. Carolan *et al.*, Phys. Rev. A **35**, 3454 (1987).
[2] R. C. Isler, Plasma Phys. Controlled Fusion **36**, 171 (1994).
[3] P. Beiersdorfer, M. Bitter, M. Marion, and R. E. Olson, Phys. Rev. A **72**, 032725 (2005).
[4] T. E. Cravens, Science **296**, 1042 (2002).
[5] V. A. Krasnopolsky, J. B. Greenwood, and P. C. Stancil, Space Sci. Rev. **113**, 271 (2004).
[6] C. M. Lisse *et al.*, Astrophys. J. **635**, 1329 (2005), and references therein.
[7] T. E. Cravens and T. I. Gombosi, Adv. Space Res. **33**, 1968 (2004).
[8] B. J. Wargelin and J. J. Drake, Astrophys. J. **578**, 503 (2002).
[9] R. F. Elsner *et al.*, J. Geophys. Res. **110**, A01207 (2005).
[10] V. Kharchenko, A. Dalgarno, D. R. Schultz, and P. C. Stancil, Geophys. Res. Lett. **33** (11), L11105 (2006).
[11] N. A. Schwadron and T. E. Cravens, Astrophys. J. **544**, 558 (2000).
[12] V. Kharchenko and A. Dalgarno, J. Geophys. Res. **105**, 18351 (2000).
[13] A. A. Hasan, F. Eissa, R. Ali, D. R. Schultz, and P. C. Stancil, Astrophys. J. Lett. **560**, L201 (2001).
[14] R. Ali *et al.*, Astrophys. J. Lett. **629**, L125 (2005).
[15] R. E. Olson and A. Salop, Phys. Rev. A **16**, 531 (1977).
[16] S. E. Butler and A. Dalgarno, Astrophys. J. **241**, 838 (1980).
[17] R. K. Janev, D. S. Belić, and B. H. Bransden, Phys. Rev. A **28**, 1293 (1983).
[18] P. C. Stancil, A. R. Turner, D. L. Cooper, D. R. Schultz, M. J. Raković, W. Fritsch, and B. Zygelman, J. Phys. B **34**, 2481 (2001).
[19] H. Ryufuku, K. Sasaki, and T. Watanabe, Phys. Rev. A **21**, 745 (1980).
[20] R. Mann, F. Folkmann, and H. F. Beyer, J. Phys. B **14**, 1161 (1981).
[21] A. Niehaus, J. Phys. B **19**, 2925 (1986).
[22] A. Itoh *et al.*, J. Phys. Soc. Jpn. **64**, 3255 (1995).
[23] S. Otranto, R. E. Olson, and P. Beiersdorfer, Phys. Rev. A **73**, 022723 (2006).
[24] P. Beiersdorfer, C. M. Lisse, R. E. Olson, G. V. Brown, and H. Chen, Astrophys. J. Lett. **554**, L99 (2001).
[25] M. Rigazio, V. Kharchenko, and A. Dalgarno, Phys. Rev. A **66**, 064701 (2002).
[26] V. Kharchenko, M. Rigazio, A. Dalgarno, and V. A. Krasnopolsky, Astrophys. J. Lett. **585**, L73 (2003).
[27] K. Dennerl *et al.*, Astron. Astrophys. **451**, 709 (2006).
[28] A. Chutjian, J. B. Greenwood, and S. J. Smith, *Applications of Accelerators in Research and Industry*, edited by J. L. Duggan and I. L. Morgan (American Institute of Physics, New York, 1999), p. 881.
[29] J. B. Greenwood, A. Chutjian, and S. J. Smith, Astrophys. J. **529**, 605 (2000).
[30] J. B. Greenwood, I. D. Williams, S. J. Smith, and A. Chutjian, Astrophys. J. Lett. **533**, L175 (2000).
[31] J. B. Greenwood, D. Williams, S. J. Smith, and A. Chutjian, Phys. Rev. A **63**, 062707 (2001).
[32] I. Čadež, J. B. Greenwood, J. A. Lozano, R. J. Mawhorter, S. J. Smith, M. Niimura, and A. Chutjian, J. Phys. B **36**, 3303 (2003).
[33] D. Bordenave-Montesquieu and R. Dagnac, J. Phys. B **25**, 2573 (1992).
[34] D. Bordenave-Montesquieu and R. Dagnac, J. Phys. B **27**, 543 (1994).
[35] T. Kusakabe, H. Yoneda, Y. Mizumoto, and K. Katsurayama, J. Phys. Soc. Jpn. **59**, 1218 (1990).
[36] R. E. Olson and M. Kimura, J. Phys. B **15**, 4231 (1982).
[37] S. J. Smith, I. Čadež, A. Chutjian, and M. Niimura, Astrophys. J. **602**, 1075 (2004).
[38] S. J. Smith, A. Chutjian, and J. A. Lozano, Phys. Rev. A **72**, 062504 (2005).
[39] B. R. Turner, J. A. Rutherford, and D. M. J. Compton, J. Chem. Phys. **48**, 1602 (1968).
[40] C. Liao, S. J. Smith, D. Hitz, A. Chutjian, and S. S. Tayal, Astrophys. J. **484**, 979 (1997)
[41] S. J. Smith, N. Djurić, J. A. Lozano, K. A. Berrington, and A. Chutjian, Astrophys. J. **630**, 1213 (2004).
[42] N. Djurić, R. Mawhorter, S. J. Smith, and A. Chutjian, XXIV Int. Conf. Phys. Photonic Electronic Collisions (Rosario, Argentina, 2005), Abstract TU094.
[43] W. E. Moddeman, T. A. Carlson, M. O. Krause, B. P. Pullen, W. E. Bull, and G. K. Schweitzer, J. Chem. Phys. **55**, 2317 (1971).
[44] T. Koopmans, Physica (Amsterdam) **1**, 104 (1933); see also A. Szabo and N. S. Ostlund, *Modern Quantum Chemistry* (Dover, Mineola, NY, 1996).
[45] P. Stancil, in the 206th American Astronomy Society Meeting, Minneapolis, MN, 2005, (unpublished), Abstract 31.21.
[46] I. Čadež, J. B. Greenwood, A. Chutjian, R. J. Mawhorter, S. J.

Smith, and M. Niimura, J. Phys. B **35**, 2515 (2002).
[47] J. B. Greenwood, R. J. Mawhorter, I. Čadež, J. Lozano, S. J. Smith, and A. Chutjian, Phys. Scr., T **110**, 358 (2004).
[48] D. Bodewits, R. Hoekstra, B. Seredyuk, R. W. McCullough, G. H. Jones, and A. G. G. M. Tielens, Astrophys. J. **642**, 593 (2006).
[49] B. Seredyuk *et al.*, Phys. Rev. A **71**, 022705 (2005).
[50] E. Bell, Ph.D. thesis, University of Colorado, Boulder, CO, 1993.
[51] K. Dennerl *et al.*, Astron. Astrophys. **451**, 709 (2006).
[52] A. Niehaus, Nucl. Instrum. Methods Phys. Res. B **23**, 17 (1987).
[53] G. Sampoll, R. L. Watson, O. Heber, V. Horvat, K. Wohrer, and M. Chabot, Phys. Rev. A **45**, 2903 (1992).
[54] H. O. Folkerts, T. Schlathőlter, R. Hoekstra, and R. Morgenstern, J. Phys. B **30**, 5849 (1993).
[55] R. J. Mawhorter *et al.* (unpublished).
[56] W. Steinmentz (private communication).